ISSN 0021-3640, JETP Letters, 2012, Vol. 95, No. 1, pp. 20–24. © Pleiades Publishing, Inc., 2012.
Original Russian Text © A.S. Fedorov, A.A. Kuzubov, T.A. Kozhevnikova, N.S. Eliseeva, N.G. Galkin, S.G. Ovchinnikov, A.A. Saranin, A.V. Latyshev, 2012, published in Pis'ma v Zhurnal Eksperimental'noi i Teoreticheskoi Fiziki, 2012, Vol. 95, No. 1, pp. 23–28.

Features of the Structure and Properties of β-$FeSi_2$ Nanofilms and a β-$FeSi_2$/Si Interface

A. S. Fedorov[a, *], A. A. Kuzubov[b], T. A. Kozhevnikova[b], N. S. Eliseeva[b], N. G. Galkin[c], S. G. Ovchinnikov[a, b], A. A. Saranin[c], and A. V. Latyshev[d]

[a] *Kirensky Institute of Physics, Siberian Branch, Russian Academy of Sciences, Krasnoyarsk, 660036 Russia*

* *e-mail: alex99@iph.krasn.ru*

[b] *Siberian Federal University, Krasnoyarsk, 660041 Russia*

[c] *Institute of Automation and Control Processes, Far East Branch, Russian Academy of Sciences, Vladivostok, 690041 Russia*

[d] *Rzhanov Institute of Semiconductor Physics, Siberian Branch, Russian Academy of Sciences, Novosibirsk, 630090 Russia*

Received October 21, 2011; in final form, November 29, 2011

The electronic, geometric, and magnetic structure of nanofilms of the β phase of iron disilicide $FeSi_2$ with the (001), (100), and (010) surfaces have been simulated through density functional calculations. A substantial reconstruction of the (001) surface terminated with silicon atoms has been observed, which was accompanied by an increase in the surface symmetry and appearance of "squares" of silicon atoms. Analysis of the electron density of states (DOS) and spin DOS projected on the contributions of layers of atoms (LSDOS) indicates that all plates have metallic properties. The main contribution near the Fermi level comes from the surface iron layers and it decreases rapidly with an increase in the distance from the surface of the plate. Analysis of the calculated effective magnetic moments of atoms shows that the surface layers in the plates have a significant magnetic moment, in particular, iron layers on the (001) surface (1.89 μ_B/atom). The moments of atoms decrease rapidly with an increase in their distance from the surface. The electron and geometric regions of a (001)Si/$FeSi_2$ interface have been studied. Analysis of the LSDOS shows that the surface conducting state mainly determined by the contribution from the near-surface silicide layers is implemented in this region. The possibility of the formation of the perfect and sharp Si/$FeSi_2$ interface has been demonstrated.

DOI: 10.1134/S0021364012010055

At present, the study of the ferromagnetic metal/nonmagnetic metal or semiconductor heterostructures has become of increasing importance because of the potentially wide applications of these nanostructures, e.g., owing to the giant magnetoresistance effect, the discovery of which was awarded the 2007 Nobel Prize in Physics. Multilayered nanostructures with alternating ferromagnetic and nonmagnetic layers have interesting properties of spin electron transport, when it can be controlled by varying the external conditions [1, 2]. When silicon is used as a semiconductor, the high spin polarization and low resistivity make these systems one of the most promising materials for spintronics [2–4]. Recently, the optical properties of semiconductor structures containing iron disilicide nanocrystallites have also been actively studied [5–8], because the transition metal silicide nanostructures can be used as light emitters and optical detectors (see [30], which is completely devoted to silicide properties). For example, iron disilicide with the β-$FeSi_2$ phase in contrast to bulk silicon has a direct band gap with the width $E_g = 0.85–0.87$ eV [10, 11]. Therefore, it has good luminescent properties in the near infrared spectral range (0.80–0.84 eV) that is important for use in fiber-optic communication lines [12, 13]. Magnetic silicide Fe_3Si in the composition of the layered $SiO_2/Fe_3Si/Si$ nanostructure was used experimentally as a magneto-optical modulator. An important advantage of various transition metal silicides is high abundance of these elements in nature. All these facts indicate that the problem of studying the formation of silicide nanolayers and interface layers at the silicon and transition metal boundary is undoubtedly topical. The variation of the electronic, magnetic, and optical properties of these structures during the transition from the crystalline silicon to the silicide structure was hardly studied experimentally because these systems are nanosized. Owing to the lack of information about the structure of the interface region, different variants of the Fe/Si interface were proposed: Fe/Se [14], Fe/Si_2 [15,16], and Fe_3/Si [17, 18]. In [19, 20], the relation between the chemical structure and magnetic properties of the interface was studied by the photoelectron spectroscopy method. It turned out that the first step to the formation of a sili-

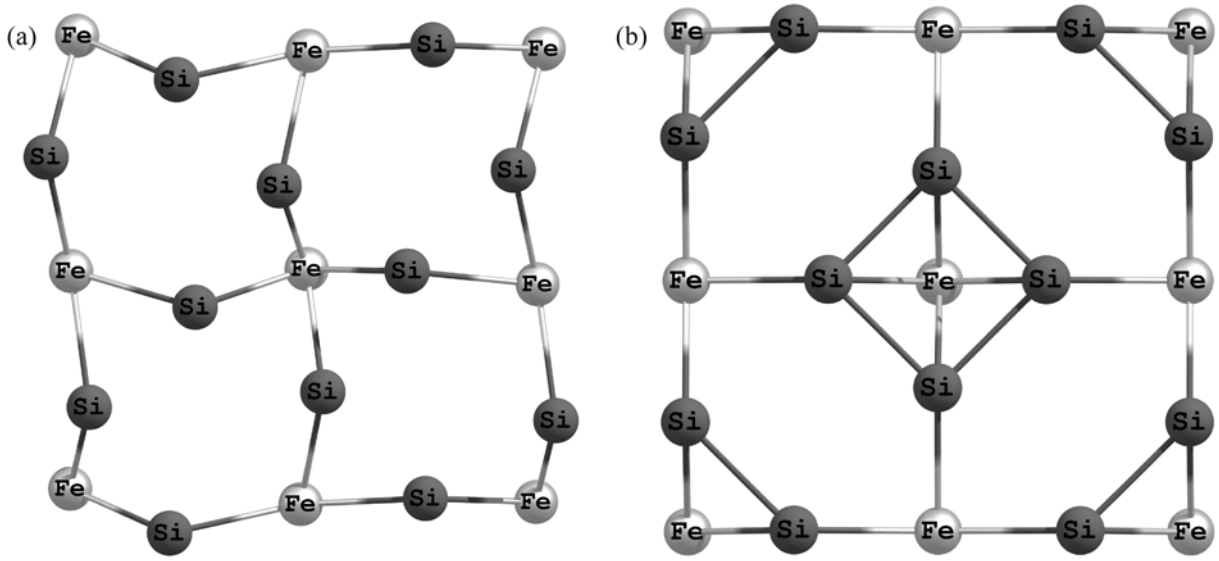

Fig. 1. (a) Unreconstructed and (b) reconstructed surfaces of the (001) plate.

cide at room temperature is the penetration of Fe atoms into the Si lattice with filling of the substitution sites [21]. In experimental work [9], the authors found the appearance of a magnetic layer of iron-enriched silicide by studying the interface between a thin β-$FeSi_2$ film and a silicon (111) substrate by transmission electron microscopy and precision magnetization measurements.

Thus, because of the lack of experimental information, the use of the ab initio theoretical calculations makes it possible to better understand the mechanisms of the formation and properties of the silicide layers and the silicon/silicide interface regions. This work is devoted to the theoretical study of the electronic and geometric structure of thin (≈15 Å thick) iron silicide films with the β-$FeSi_2$ phase and the region of their interface with the silicon (001) surface. This study makes it possible to better understand the mechanism of the reconstruction of the free surface of the β-$FeSi_2$ crystal and to determine the change in the surface electronic and magnetic structure. The experimental data on the fabrication of iron disilicide nanoparticles in the silicon matrix and high-resolution electron microscopy data are presented, which confirm the possibility of the epitaxial growth of disilicide on the silicon surface.

To perform the ab initio theoretical study of the structures in question, we used the pseudopotential method based on the density functional formalism [22, 23] and the generalized gradient approximation with a plane-wave basis set proposed by Perdew and Wang (PW91) in [24]. The calculations were performed with the use of the licensed VASP 5.2 (Vienna ab initio simulation package) package [25–27]. In this program, the ultrasoft Vanderbilt pseudopotentials [28] are used in order to effectively reduce the number of basis plane waves and, correspondingly, to increase the calculation speed. They make it possible to substantially reduce the maximum kinetic energy of plane waves (E_{cutoff}). This reduces the basis size and strongly accelerates the calculations. In all calculations, E_{cutoff} was chosen to be 237.5 eV. A set of k points in a mesh ($2 \times 2 \times 1$) chosen with the help of the Monkhorst–Pack scheme proposed in [29] was used for integration over the first Brillouin zone (1BZ) because of the large sizes of the supercells. To optimize the geometry of nanoplates, the atom positions were optimized until the absolute values of forces acting on all atoms became less than 0.05 eV/Å.

We analyzed the electronic and geometric structures of nanofilms of the β-$FeSi_2$ composition with the (001), (100), and (010) surfaces. In order to study the effect of the nature of the surface atoms, each plate was chosen to be limited by iron atoms on one side and silicon atoms on the other side. All studied nanofilms were simulated by introducing periodic conditions for a supercell in the film plane and introducing a vacuum gap in the perpendicular direction (slab geometry). The vacuum gap was 10 Å, which guaranteed the absence of chemical interactions between the neighboring periodic plates. The sizes of the supercells of the silicide plates with the (001), (100), and (010) surfaces were $15.6 \times 15.7 \times 18.3$, $12.0 \times 15.7 \times 19.8$, and $15.6 \times 13.9 \times 19.8$ Å, respectively, which corresponded to the $2 \times 2 \times 2$ basis vectors for the unit cell of β-$FeSi_2$, which included 48 atoms. This orthorhombic cell after the optimization over the volume had the dimensions of $9.87 \times 7.87 \times 7.85$ Å, which deviate from the experimental values by less than 1%. The number of atomic

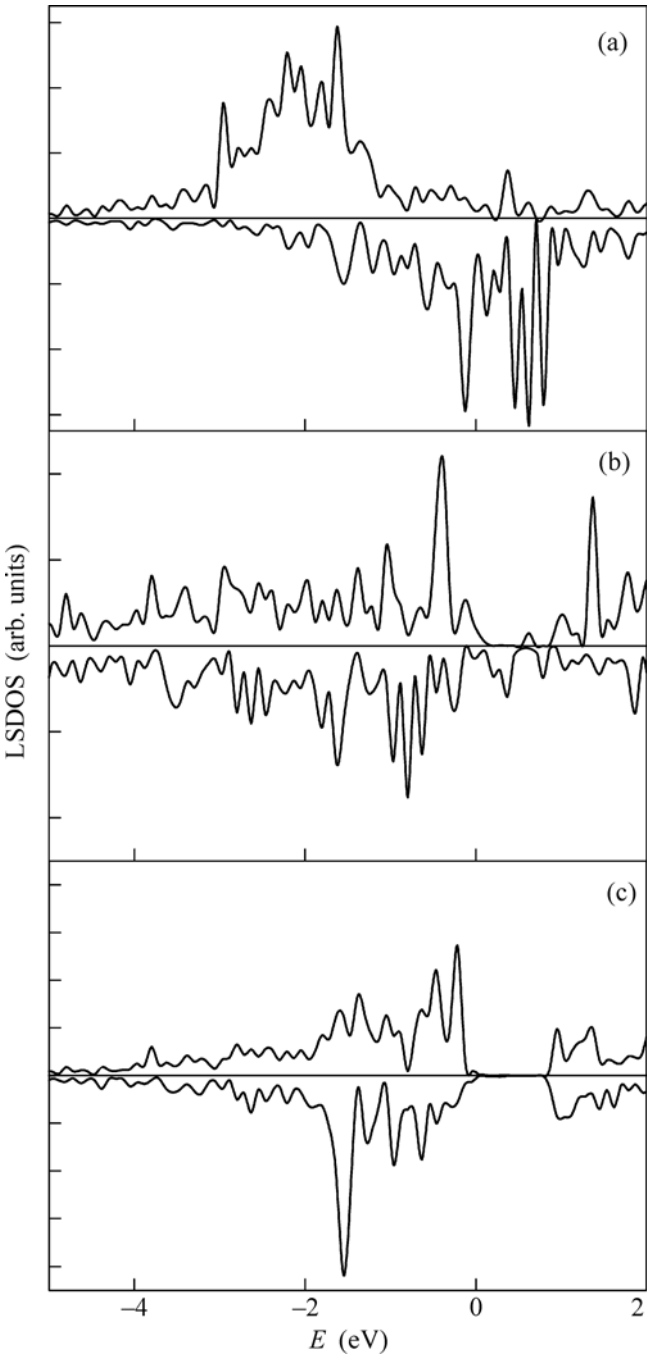

Fig. 2. Projected spin densities of states of the (a) surface Fe layer, (b) central Fe layer, and (c) surface Si layer on the opposite surface for the (001) plate. Energies are measured from the Fermi level.

layers over the thickness in the plates was 16 for the (001) film and 8 for the (100) and (010) films.

It was established during the optimization of all three nanofilms that the (001) film experiences a substantial surface reconstruction from the surface terminated with silicon atoms. This reconstructed surface is shown in Fig. 1b. It can be seen that the fourfold axis

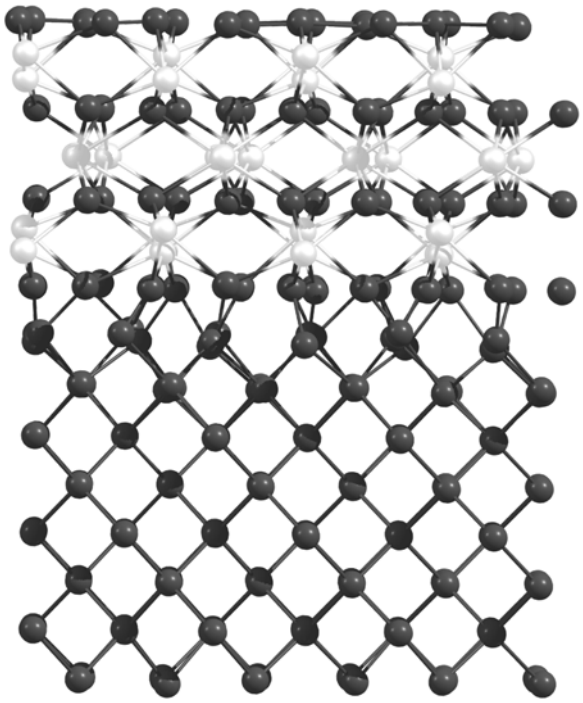

Fig. 3. Optimized geometry of the silicon/silicide interface. Silicon atoms are denoted by a darker color.

appears for the surface symmetry with the formation of "squares" of silicon atoms. This reconstruction can be explained by the tendency of the surface silicon atoms to reduce the number of dangling bonds by forming new covalent bonds between each other and by adequate distances between the silicon atoms on this surface. For comparison, Fig. 1a shows the unreconstructed surface.

For all other nanofilms and for the other (001) surface, covered by Fe atoms, the displacement of atoms did not exceed 0.1 Å. Therefore, no substantial reconstruction took place, although the distance between the surface layers always decreased. This partially redistributed the electron density of dangling bonds to an increase in the density of the subsurface bonds and thus decreased the total energy of the system. The absence of reconstruction in these cases is explained by the absence of the surface layer of silicon atoms.

The calculation of the electron density of states (DOS) indicates that all three nanofilms have metallic properties. To analyze the properties of individual atomic layers chosen parallel to the surface plane, we performed the procedure of projecting the total spin density of states (SDOS) on the contributions from the atoms belonging to each of these layers (layered SDOS (LSDOS)) (see Fig. 2). Figure 2 shows the LSDOS for (a) the surface layer of iron atoms in the (001) plate, (b) the central layer of iron atoms, and (c) surface layers of silicon atoms on the opposite surface.

It can be seen in the figure that the main contribution to the total DOS on the Fermi level comes from the surface iron layer. The strong magnetic polarization of this layer is observed. To analyze the magnetic properties of all plates in more detail, we calculated their total magnetizations, which were 0.10, 0.04, and 0.02 μ_B/atom for the (001), (100), and (010) plates, respectively. To determine the contribution to the total magnetization from individual atomic layers by the method similar to the above projection procedure, we calculated the total magnetic moments of iron and silicon atoms lying on the surfaces of all three plates.

It can be seen from these data that the magnetic moment of the films is due to the surface layers, in particular, the layers of iron atoms in the (001) film. The moments of atoms decrease rapidly in the direction to the center of the plates.

In addition, we studied the electronic structure and geometry of the silicon (001) surface/β-$FeSi_2$ silicide (001) surface interface region. To find the equilibrium geometric interface structure, we used the ab initio molecular dynamics (MD) method with the damping procedure; i.e., fictitious friction forces were introduced during the calculation of the dynamics and forces acting on the atoms. The friction forces gradually decelerate atoms and thus decrease the kinetic energy (temperature) of the system. As a result, the temperature of the system decreases gradually from a chosen value of 2000 K to ≈0 K. For this reason, atoms stick near the minimum of the total energy of the system. This method, which was tested earlier for the description of the structure of amorphous silicon, made it possible to determine the equilibrium geometry of the interface region, where the order of the positions of atoms was not known in advance. The final geometry of the interface is shown in Fig. 3. We performed experiments on the synthesis of β-$FeSi_2$ nanoparticles embedded into the crystalline silicon matrix. The β-$FeSi_2$ nanocrystallites were fabricated at the Institute of Automation and Control Processes, Far East Branch, Russian Academy of Sciences, according to the same scheme. At the first stage, the iron disilicide islands were formed on the atomically pure Si(100) surface. The β-$FeSi_2$ islands were formed by the reactive epitaxy method by depositing an iron layer (0.2 nm) on a silicon substrate at a temperature of 475°C at a rate of 0.8 nm/min. Then, the islands were covered by an epitaxial silicon layer of various thicknesses (≈100 nm), which was grown at a substrate temperature of 700°C and a silicon deposition rate of 3–20 nm/min. The silicide islands were collected in nanocrystals with different shapes during the growth of the coating silicon layer. To form a multilayered structure, the first and second stages were repeated as many times as necessary. This sample was additionally annealed at a temperature of 850°C for 8 h to anneal the formed defects. The exact conjugation and epitaxial relations could not be determined from the data of high-resolution transmission electron microscopy performed at the Rzhanov Institute of Semiconductor Physics, Siberian Branch, Russian Academy of Sciences, since the Fourier image contained few additional reflections. Nevertheless, it was established that the β-$FeSi_2$/Si interface layer is sufficiently perfect and thin (see Fig. 4).

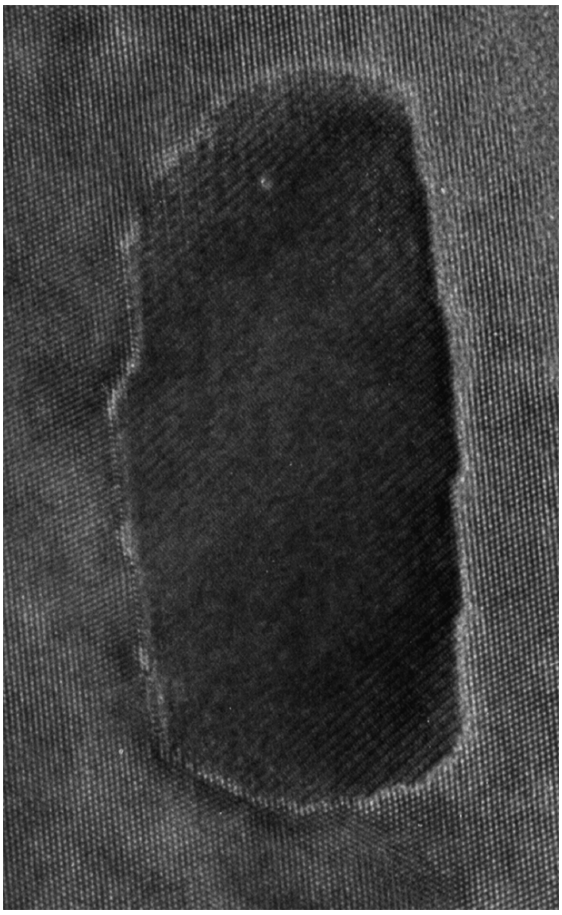

Fig. 4. Transmission electron microscopy photo of the β-$FeSi_2$ particle embedded in the silicon matrix.

To summarize, it has been shown by means of the density functional calculations that the β-$FeSi_2$ nanoplates with the (001), (100), and (010) surfaces have surface conductivity mainly owing to the surface iron atoms. It was found that the surface layers have a large magnetic moment that decreases rapidly toward the center of the plates. Substantial reconstruction of the (001) surface terminating with the silicon atoms was also found. It was accompanied by an increase in the surface symmetry and an appearance of squares of silicon atoms. The study of the electron structure and geometry of the silicon (001) surface/β-$FeSi_2$ silicide (001) surface interface has revealed that the interface region, as well as silicide plates, has surface conductivity and is perfect and thin. The conclusions about the

Average magnetic moments μ_{aver} of Fe and Si atoms in the layers with the number N or alternating atoms (Alt.) in nanofilms with the (001), (100), and (010) surfaces

Surface	N	μ_{aver}	Atom	Surface	N	μ_{aver}	Atom
	1	1.893		(100)	1	0.202	Alt.
	2	–0.055			2	–0.031	Alt.
	3	–0.052			3	–0.007	Alt.
	4	–0.003			4	0.001	Alt.
	5	–0.026			5	–0.001	Alt.
(001)	6	0.001			6	–0.010	Alt.
	7	0.000			7	–0.000	Alt.
	8	0.000			8	0.138	Alt.
	9	0.003		(010)	1	0.073	Alt.
	10	0.000			2	–0.026	Alt.
	11	–0.021			3	–0.005	Alt.
	12	–0.002			4	0.000	Alt.
	13	0.061			5	0.003	Alt.
	14	–0.015			6	–0.000	Alt.
	15	0.677			7	–0.030	Alt.
	16	0.012			8	0.112	Alt.

interface geometry have been confirmed by the experiments performed.

We are grateful to the Interdepartmental Supercomputer Center, Russian Academy of Sciences (Moscow), for the access to the MBC-100K cluster and to the Institute of Computational Modeling, Siberian Branch, Russian Academy of Sciences, for the use of their supercomputers for performing all calculations. This work was supported by the Siberian Branch, Russian Academy of Sciences (integration project no. 22); the Russian Foundation for Basic Research (project no. 11-02-92001); the Ministry of Education and Sciences of the Russian Federation (state contract no. 2011-1.2.1-207-018-002, federal program "Human Capital"); and the Presidium of the Russian Academy of Sciences (project no. 27.10).

REFERENCES

1. I. Zutic, J. Fabian, and S. D. Sarma, Rev. Mod. Phys. **76**, 323 (2004).
2. H. Wu, P. Kratzer, and M. Scheffler, Phys. Rev. B **72**, 144425 (2005).
3. A. Horsfield, S. Kenny, and H. Fujitani, Phys. Rev. B **64**, 245332 (2001).
4. G. Rangelov and Th. Fauster, Surf. Sci. **365**, 403 (1996).
5. S. Murase et al., J. Crystal Growth **301–302**, 676 (2007).
6. N. G. Galkin et al., J. Nanosci. Nanotechnol. **8**, 527 (2008).
7. N. G. Galkin et al., Tech. Phys. **53**, 224 (2008).
8. N. G. Galkin et al., Appl. Surf. Sci. **166**, 113 (2000).
9. A. N. Hattori, K. Hattori, K. Kodama, et al., Appl. Phys. Lett. **91**, 201916 (2007).
10. N. E. Christensen, Phys. Rev. B **42**, 7148 (1990).
11. A. B. Filonov, D. B. Migas, V. L. Shaposhnikov, et al., J. Appl. Phys. **83**, 4410 (1998).
12. K. J. Reeson, J. S. M. Harry, D. Leong, et al., Microelectron. Eng. **50**, 223 (2000).
13. B. Shuller, R. Carius, S. Lenk, and S. Mantl, Microelectron. Eng. **60**, 205 (2000).
14. H. von Kanel et al., Phys. Rev. B **45**, 13807 (1992).
15. G. Crecelius, Appl. Surf. Sci. **65–66**, 683 (1993).
16. E. V. Chubina et al., Thin Solid Films **247**, 39 (1994).
17. J. M. Gallego et al., Phys. Rev. B **46**, 13339 (1992).
18. J. Alvarez et al., Phys. Rev. B **45**, 14042 (1992).
19. R. Klasges et al., Phys. Rev. B **56**, 10801 (1997).
20. I. I. Pronin, M. V. Gomoyunova, D. E. Malygin, et al., Phys. Solid State **50**, 553 (2008).
21. A. Mascaraque et al., Phys. Rev. B **55**, R7315 (1997).
22. G. Kresse and D. Joubert, Phys. Rev. **59**, 1758 (1999).
23. K. Laasonen, A. Pasquarello, R. Car, et al., Phys. Rev. B **47**, 10142 (1993).
24. J. P. Perdew and Y. Wang, Phys. Rev. B **45**, 13244 (1992).
25. G. Kresse and J. Hafner, Phys. Rev. B **48**, 13115 (1993).
26. G. Kresse and J. Furthmöller, Phys. Rev. **54**, 11169 (1996).
27. G. Kresse and J. Furthmöller, Comput. Mater. Sci. **6**, 15 (1996).
28. D. Vanderbilt, Phys. Rev. B **41**, 7892 (1990).
29. H. J. Monkhorst and J. D. Pack, Phys. Rev. B **13**, 5188 (1976).
30. Physics Procedia, **11** (2011).

Translated by L. Mosina